AGU PUBLICATIONS

JGR

Journal of Geophysical Research: Oceans

RESEARCH ARTICLE

10.1002/2016JC012318

Observations and a linear model of water level in an interconnected inlet-bay system

Alfredo L. Aretxabaleta[1], Neil K. Ganju[1], Bradford Butman[1], and Richard P. Signell[1]

[1]U.S. Geological Survey, Woods Hole Coastal and Marine Science Center, Woods Hole, Massachusetts, USA

Key Points:
- We analyze observed water levels in the bays of southern Long Island to characterize changes in bay response to offshore fluctuations
- Temporal changes in tides and transfer of offshore water level reflected inlet dredging and possibly the changing size of the Wilderness Breach
- An analytical model predicts water level response in all bays including those that lacked observational data

Correspondence to:
A. L. Aretxabaleta,
aaretxabaleta@usgs.gov

Citation:
Aretxabaleta, A. L., N. K. Ganju, B. Butman, and R. P. Signell (2017), Observations and a linear model of water level in an interconnected inlet-bay system, *J. Geophys. Res. Oceans*, *122*, 2760–2780, doi:10.1002/2016JC012318.

Received 6 SEP 2016
Accepted 12 FEB 2017
Accepted article online 15 FEB 2017
Published online 4 APR 2017

Abstract A system of barrier islands and back-barrier bays occurs along southern Long Island, New York, and in many coastal areas worldwide. Characterizing the bay physical response to water level fluctuations is needed to understand flooding during extreme events and evaluate their relation to geomorphological changes. Offshore sea level is one of the main drivers of water level fluctuations in semienclosed back-barrier bays. We analyzed observed water levels (October 2007 to November 2015) and developed analytical models to better understand bay water level along southern Long Island. An increase (~0.02 m change in 0.17 m amplitude) in the dominant M_2 tidal amplitude (containing the largest fraction of the variability) was observed in Great South Bay during mid-2014. The observed changes in both tidal amplitude and bay water level transfer from offshore were related to the dredging of nearby inlets and possibly the changing size of a breach across Fire Island caused by Hurricane Sandy (after December 2012). The bay response was independent of the magnitude of the fluctuations (e.g., storms) at a specific frequency. An analytical model that incorporates bay and inlet dimensions reproduced the observed transfer function in Great South Bay and surrounding areas. The model predicts the transfer function in Moriches and Shinnecock bays where long-term observations were not available. The model is a simplified tool to investigate changes in bay water level and enables the evaluation of future conditions and alternative geomorphological settings.

Plain Language Summary We analyze water level observations in the bays of southern Long Island (Jamaica Bay, Great South Bay and connected bays) to determine how the bays respond to the conditions in the open ocean. We focus especially on changes in time in the tides and in the response to storms. The tides and the water level relationship with offshore have been changing slightly in recent years (2008–2015). The changes occur at times during or immediately after inlet dredging and also as a result of the changing dimensions of a breach through Fire Island caused by Hurricane Sandy. We propose a simple model that takes into account the inlet and bay dimensions and friction in the inlet channels to predicts water level response to tides and storms in all bays including those for which long-term observational data were not available.

1. Introduction

Coastal bays or back-barrier estuaries are common features along the U.S. east coast. They are shallow coastal embayments separated from the ocean by extensive systems of barrier islands. Bay and mainland flood risk during extreme events has severe socioeconomic repercussions [*Nicholls et al*., 2007]. Offshore sea level is often the main driver of water level fluctuations in semienclosed back-barrier bays during storms and also controls tidal exchanges [*Keulegan*, 1967; *Chuang and Swenson*, 1981; *Garvine*, 1985]. Long-lasting fluctuations (e.g., storm surge, sea level rise) are more effectively transferred from the offshore into the bays than short-period fluctuations (e.g., semidiurnal tides). Smaller inlets restrict transfer of offshore fluctuations into bays [*Keulegan*, 1967]. If offshore water level were maintained for long periods, enough water would flow through the inlets, overcoming the frictional restrictions, and the water level in the bays would match the offshore level [*Chuang and Swenson*, 1981; *Aretxabaleta et al*., 2014].

The response of bay water level to offshore forcing has been previously studied in a number of coastal settings. *Wong and Wilson* [1984] found that the substantial subtidal sea level fluctuations in Great South Bay were forced primarily by a strong bay-shelf coupling effect. In Lake Pontchartrain, a similar bay-inlet system,

Chuang and Swenson [1981] found that coupled coastal ocean-bay response was dominant at subtidal frequencies. *Garvine* [1985] showed using a simple analytical model that remote effects dominate over local effects in estuarine systems with large enough openings. *Wong and DiLorenzo* [1988] found that inland bays in the Delaware Bay system were forced primarily by coastal sea level fluctuations at both tidal and subtidal frequencies.

During large storm events, the bay system is affected by the offshore storm surge but the barrier island system prevents the water level in the back-barrier bays from fully matching the offshore level, as the size of the inlets that constrain the flow remains mostly unchanged and frictional forces limit the exchange. Only when added connections between ocean and bay are created (breaching) and/or when the barrier island is overtopped (overwash), is there additional transfer from the ocean side. In the Fire Island system, the *U.S. Army Corps of Engineers* [2001] suggested that breaching of the barrier island could increase tidal range as much as 0.3 m along the mainland in Great South Bay with larger effects on storm surge (0.6 m higher water levels). *Cañizares and Irish* [2008] compared simulations with/without breaching and overwash during the 1938 Hurricane and suggested that the effect of Moriches Inlet on the flooding of Moriches Bay was as large 0.75–1 m of excess water level in some locations. *van Ormondt et al*. [2015] suggested a much lower impact of breaching and overwash (0.1 m additional water level) in a simulation of Great South Bay during Hurricane Sandy.

Hurricane Sandy caused record flooding along the coast of the northeastern U.S. Overwash and subsequent breaching of the Long Island barrier islands during Sandy resulted in geomorphic change and new inlets across Fire Island, New York, at Cupsoque County Park (inlet closed November 2012), at Smith Point County Park (inlet closed November 2012), and at Old Inlet south of Bellport, New York (inlet open as of September 2016). In a previous study, *Aretxabaleta et al*. [2014] showed that the water level transfer function in an analysis extending from October 2007 to October 2013 did not show significant differences between before and after Hurricane Sandy conditions.

In this study, we analyze observed water level in the bays of southern Long Island to characterize temporal changes in bay response to offshore fluctuations. A analytical model with linear friction and idealized inlet geometry is introduced to explore the dominant factors affecting water level in bays, reproduce the transfer of water level from offshore, provide approximations to the water level response in bays that lacked observational data, and allow for the examination of alternative response scenarios.

2. Regional Description

The study area is in southern Long Island, New York along the Atlantic Ocean (Figure 1). The area spans more than 120 km of bays and barrier islands, consisting of four islands and six inlets that separate the

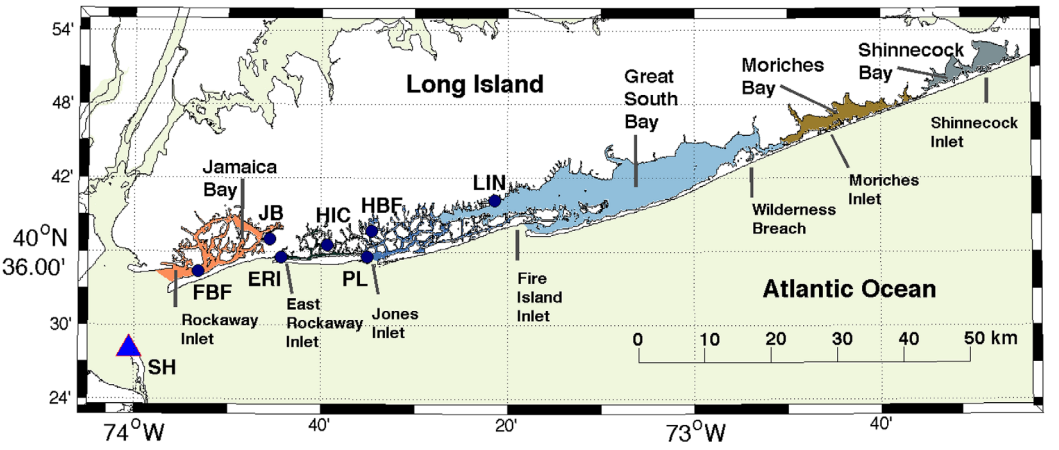

Figure 1. Map of southern Long Island showing bays and inlets, the locations of water level stations inside the bays (dark blue circles), and the offshore proxy at Sandy Hook (SH, blue triangle). See Table 1 for key to station abbreviations. The Montauk Point NOAA station is at the eastern end of Long Island, off this map.

shallow interconnected bays to the north from the Atlantic Ocean. The main bays are Jamaica Bay (connected to the ocean by Rockaway Inlet), Great South Bay (connected to the ocean by Fire Island Inlet and other smaller inlets), Moriches Bay (connected to the ocean through Moriches Inlet), and Shinnecock Bay (connected to the ocean by Shinnecock Inlet). These bays have widths that vary from a few hundred meters to 8 km. They are separated from each other by narrow connections except for Jamaica Bay, which is not joined with the bays to the east.

Prior to Hurricane Sandy, six inlets bisected the barrier islands. From west to east, these inlets were: Rockaway, East Rockaway, Jones, Fire Island, Moriches, and Shinnecock. The first four inlets predate the earliest available surveys of 1825, while the remaining two inlets were formed in the twentieth century. All inlets migrated naturally until arrested by jetties and dredging in the later part of the last century [*U.S. Army Corps of Engineers*, 2001]. During Hurricane Sandy, a new inlet (Wilderness Breach hereafter) was opened by the storm in the area of the Fire Island High Dune Wilderness at Old Inlet south of Bellport and remains open to-date.

The study area (Figure 1) can be separated into a set of six bay systems mainly controlled by their nearest inlet. From west to east, the bay systems are: Jamaica Bay, East Rockaway Inlet bay system, Jones Inlet bay system, Great South Bay, Moriches Bay, and Shinnecock Bay.

Jamaica Bay has an area of approximately 50 km^2 with a mean depth of 4 m. The bay connects with the ocean to the west through Rockaway Inlet. The inlet has an average depth across the entire inlet of about 5 m with large spatial differences ranging from about 7 m along the axis of the channel (being as deep as 16 m off Floyd Bennett Field) and less than half a meter on the shoals. The bay contains numerous salt marsh islands that are being lost at the rate of 0.1–0.16 $km^2\ yr^{-1}$ [*Hartig et al.*, 2002] affecting the inundated area of the bay.

The East Rockaway Inlet Bay system has an area of approximately 45 km^2 with a mean depth of over 2 m. The bay system comprises multiple small bays and channels. The bay system is connected to the ocean mainly through East rockaway Inlet and to adjacent bay system (dominated by Jones Inlet) predominantly though Reynolds Channel.

The Jones Inlet bay system has an area of approximately 20 km^2 with a mean depth of about 2 m. The system includes the bays between the East Rockaway Inlet bay system and Great South Bay. The system connects to the ocean through Jones Inlet and is also connected to Great South Bay to the east. There was a large dredging project of Jones Inlet in December 2007 to March 2008 (491,000 m^3 of sand removed) to improve navigation safety and another project of similar magnitude (520,000 m^3) in March–May 2014 to mitigate the effects of Hurricane Sandy.

Great South Bay (GSB, Figure 1) is a shallow (average depth is 1.3 m), long (around 40 km), and narrow (between 2.5 and 8 km) bay and is the largest bay in southern Long Island (approximately 250 km^2). The main connection with the ocean is directly through Fire Island Inlet, located at the western end of Fire Island. Great South Bay also connects to the ocean through Moriches Bay to the east and the Jones Inlet bay system to the west. Fire Island Inlet has existed continuously since at least the late 1600s [*Johnson*, 1983] but was migrating westward until stabilization around 1950. Fire Island Inlet was dredged in 2008 (474,000 m^3 of sand removed between December 2007 and March 2008), 2013 (646,000 m^3 between February and April 2013), and 2014 (1,758,000 m^3 of sand removed between November 2013 and March 2014).

Hurricane Sandy caused two breaches on Fire Island: one at Old Inlet (Wilderness Breach) and another in Smith Point County Park. Closure of the breach at Smith Point County Park was completed in November 2012. The breach within Fire Island National Seashore's wilderness area could not be immediately closed due to protective stipulations in the Park. The National Park Service (NPS) monitored the breach to determine if the breach would close naturally. Between January and March 2013, a series of winter storms caused the new inlet to migrate west and its channel deepened. The cross-sectional area of the inlet grew from approximately 100 m^2 after the storm (December 2012) to values oscillating between 300 and 400 m^2 (February–November 2013) and to maximum areas over 600 m^2 in May and October 2014. In June 2014, it decreased to values less than 500 m^2. The last measurements collected in July 2015 showed areas around 450 m^2 (http://po.msrc.sunysb.edu/GSB/).

Moriches Bay has an area of about 35 km^2 and an average depth of 1.7 m. It connects to the ocean through Moriches Inlet, which was formed by a Nor'easter in 1931 splitting Westhampton Island from Fire Island.

Shinnecock Bay is the eastern-most bay along the outer barrier bay system, with an area of about 30 km^2, and a average depth of 1.8 m. The main connection with the ocean is through Shinnecock Inlet, which was formed by the 1938 hurricane.

3. Observations and Methods

Water levels measured at eight stations in the southern Long Island region (Figure 1 and Table 1) are used in this study. The stations started recording in October 2007 except Hog Island Channel, which began in 2010, and Sandy Hook, a long-term NOAA water level station operational since 1910. Most of the analysis uses the 2007–2015 data sets (5 years before Hurricane Sandy and 3 years after).

The low-frequency offshore water level exhibits small horizontal differences along the length of Long Island with coherence squared between Sandy Hook (SH) and Montauk Point (easternmost point of Long Island) being greater than 0.9 for most subtidal frequencies and transfer function being close to one [*Wong and Wilson*, 1984]. The coherence and transfer coefficient between pressure observations at a station on the inner-shelf from December 1999 to April 2000 [*Butman et al.*, 2003] and SH water levels were also close to unity. The SH gauge is located in Raritan Bay and is connected with the adjacent shelf by a 8 km wide and over 10 m deep opening. The high coherence with offshore observations and the deep and broad connection to offshore justify using Sandy Hook observations as a proxy for offshore water level along the southern coast of Long Island.

Bathymetry to calculate bay areas and inlet dimensions was obtained from NOAA (https://www.ngdc.noaa.gov/mgg/coastal/crm.html) and updated with recent (2012–2014) bathymetric surveys by U.S. Geological Survey [*Brownell et al.*, 2015]. The average values used in the study are included in Table 2. The width and depth of the inlets were estimated by assuming a single channel of uniform size that represented the average of multiple cross sections. The length of the channel in some inlets extends beyond the island coastline into the bay to include shallow regions in the proximity of the inlet. The chosen length cutoff was the cross section for which the area in the deeper part of the channel was equal to the area in the shallow part of the cross section.

The water level spectra and transfer functions between offshore and bay water level were calculated using a Hanning 29 day window with overlapping (50%) data segments. The length of the window was chosen to provide estimates near the main tidal frequencies. Spectral transfer functions between water levels offshore (input, SH) and in the bays (output) were computed to determine the bay response to offshore forcing. *Bendat and Piersol* [1986] provided a formulation to estimate the uncertainty envelopes for the transfer function. A harmonic analysis using T_Tide [*Pawlowicz et al.*, 2002] was conducted for monthly (October 2007 to October 2015) and yearly (from 1 November to 30 October) intervals to provide estimates of the changing tidal amplitudes in time. Tidal constituent inference [*Forrester*, 1986] was necessary for the monthly harmonics based on the ratios obtained from the yearly analysis.

Table 1. Sites of Water Level Observations[a]

Site Name (Abbreviation)	Operator/Site ID	Inlet/Bay	Datum	Adjustment to NAVD88 (m)
Sandy Hook, NJ (SH)	NOAA 8531680	Offsshore proxy	MSL	0.07
Rockaway Inlet Near Floyd Bennett Field, NY (FBF)	USGS 01311875	Rockaway Inlet	NGVD29	0.34
Jamaica Bay at Inwood, NY (JB)	USGS 01311850	Jamaica Bay	NGVD29	0.34
East Rockaway Inlet at Atlantic Beach, NY (ERI)	USGS 01311145	East Rockaway Inlet	NGVD29	0.34
Hog Island Channel at Island Park, NY (HIC)	USGS 01311143	Reynolds, Broad, Hog Island Channels	NGVD29	0.34
Reynolds Channel at Point Lookout, NY (PL)	USGS 01310740	Jones Inlet	NGVD29	0.34
Hudson Bay at Freeport, NY (HBF)	USGS 01310521	Jones Bay/Middle Bay	NGVD29	0.35
Lindenhurst, Great South Bay, NY (LIN)	USGS 01309225	Great South Bay	NGVD29	0.36

[a]Data were retrieved for 1 October 2007 to 1 November 2015. National Oceanic and Atmospheric Administration (NOAA); U.S. Geological Survey (USGS). Information on instrumentation type, sampling, and quality control methodologies from the USGS stations is available at water.usgs.gov.

Table 2. Dimensions of the Inlets and Depth and Area of the Bays[a]

	Mean Depth (m)	Mean Width (m)	Mean Length (m)
Rockaway Inlet	3.3–7	935–1210	2930–4500
East Rockaway Inlet	2.9–3	182–230	3540–6520
Jones Inlet	2.8–9	637–664	1960
Fire Island Inlet	3.1–10 (6.2)	596 (540)	6030
Wilderness Breach	1.5–3	305–510	335–1050
Moriches Inlet	1.9–5 (6.0)	246 (244)	550–800
Shinnecock Inlet	1.1–2.3 (7.2)	251 (244)	460
	Mean Depth (m)	Mean Area (km^2)	
Jamaica Bay	4.1	49.1	
Reynolds, Broad, Hog Island Channels	2.3	45.3	
Jones Bay/Middle Bay	2.1	19.9	
Great South Bay	1.3	240.6–265 (290)	
Moriches Bay	1.7	36.1–38 (31)	
Shinnecock Bay	1.8	29.5 (42)	

[a]The average inlet width and length were estimated from images in Google Earth (2015) and the average depth (across the entire inlet) from NOAA Coastal Relief Model data (https://www.ngdc.noaa.gov/mgg/coastal/crm.html) updated with local USGS information where available [*Brownell et al.*, 2015]. The values in parenthesis are previous estimates of the maximum depth and width of the inlet computed from U.S. Army Corps of Engineers condition surveys collected in the late 1990s and the bay areas from NOAA navigation charts and GEODAS 2007 database [from *Irish and Cañizares*, 2009].

4. Two-Inlet Analytical Model

The bay response to ocean sea level forcing can be represented using a simple analytical model of a generic bay connected to the offshore by two separate inlets (Figure 2a). The analytical model is designed as a simplification of the water level exchange between the offshore and Great South Bay through Fire Island Inlet and the Wilderness Breach (after Hurricane Sandy). The model assumes that the bay water level responds as a level surface to ocean forcing from the inlets and thus is limited to bays with modest horizontal extent. The approach is an extension of the formulation proposed by *Chuang and Swenson* [1981] for a single inlet connecting to a bay. This model is mostly appropriate for the examination of the first-order response of the bay to ocean fluctuations, as local forcing in the bay is not included.

The along-channel depth-averaged momentum equation for the first and second channel (inlets) based on the balance between frictional effects and the elevation gradient between offshore and bay are

$$\frac{\partial u_1}{\partial t} = g\frac{(\eta_o - \eta_e)}{L_1} - \frac{r_1}{h_1}u_1 \quad \text{and} \quad \frac{\partial u_2}{\partial t} = g\frac{(\eta_o - \eta_e)}{L_2} - \frac{r_2}{h_2}u_2$$

and the continuity equation for the bay/channel system based on the changing volume of the bay as water flows through the inlets is

$$A_e\frac{\partial \eta_e}{\partial t} = h_1 W_1 u_1 + h_2 W_2 u_2$$

where A_e is the surface area of the bay; η_e the sea level in the bay; η_o the sea level in the ocean; with h_n the water depth; W_n the width and L_n the length of channel n and r is the linear drag coefficient. Thus, the linearized bottom stress is $\tau_b{}^n = r_n u_n$, for n = 1,2.

Assuming $\eta = \eta e^{i\omega t}$ and $u = ue^{i\omega t}$ yields the system of equations:

$$i\omega A_e \eta_e = h_1 W_1 u_1 + h_2 W_2 u_2$$

$$u_n = g\frac{(\eta_o - \eta_e)}{L_n\left(\frac{r_n}{h_n} + i\omega\right)}$$

for n = 1,2.

The ratio between linear friction and depth of the channel, $\omega_f = \frac{r_n}{h_n}$, can be defined as the characteristic frequency of frictional dissipation in the channel. The frequency of frictional dissipation is the inverse of the frictional adjustment time [*Csanady*, 1981] from linear drag. The $i\omega$ term represents the phase shift between the frictional effect and the pressure forcing. Substituting into the continuity equation yields

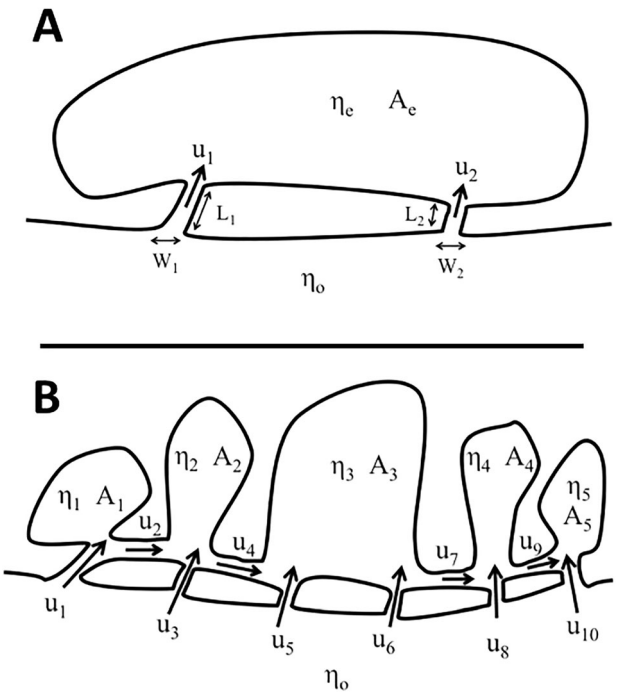

Figure 2. Schematic diagrams of the ocean-inlet-bay system: (a) with two inlets between the bay and the ocean; and (b) with six inlets between the bays and the ocean and 5 bays. A_j is the surface area of the bays; η_j the sea level in the bays; η_o the sea level in the ocean; and u_j is the velocity through channel j. The correspondence in Figure 2b with the real bay system includes areas from the bays (East Rockaway bay system, A_1; Jones Inlet bay system, A_2; Great South Bay, A_3; Moriches Bay, A_4; Shinnecock Bay, A_5), flow through inlets (East Rockaway Inlet, u_1; Jones Inlet, u_3; Fire Island Inlet, u_5; Wilderness Breach, u_6; Moriches Inlet, u_8; and Shinnecock Inlet, u_{10}), and flow between bays (Reynolds Channel, u_2; Hudson Channel, u_4; Smith Point Channel, u_7; Quogue Canal, u_9).

$$i\omega A_e\eta_e = h_1W_1g\frac{(\eta_o-\eta_e)}{L_1\left(\frac{r_1}{h_1}+i\omega\right)} + h_2W_2g\frac{(\eta_o-\eta_e)}{L_2\left(\frac{r_2}{h_2}+i\omega\right)}$$

The resulting expression for the water level in the interior of the bay is

$$\eta_e = \eta_o\left\{\frac{\frac{h_1W_1g}{L_1\left(\frac{r_1}{h_1}+i\omega\right)}+\frac{h_2W_2g}{L_2\left(\frac{r_2}{h_2}+i\omega\right)}}{i\omega A_e+\frac{h_1W_1g}{L_1\left(\frac{r_1}{h_1}+i\omega\right)}+\frac{h_2W_2g}{L_2\left(\frac{r_2}{h_2}+i\omega\right)}}\right\}.$$

The denominator in the expression provides an approximation to the natural frequency of the bay in the absence of friction (Helmholtz frequency):

$$i\omega A_e+\frac{h_1W_1g}{L_1(i\omega)}+\frac{h_2W_2g}{L_2(i\omega)}=0$$

then, $\omega_N=\left(\frac{h_1W_1gL_2+h_2W_2gL_1}{A_eL_1L_2}\right)^{1/2}$ is the natural frequency since the response of the bay will reach infinity as $\omega \to \omega_N$. Several studies described the water level conditions for fluctuations near the Helmholtz frequency in single inlet-single bay systems [*Sorensen and Seelig*, 1977; *Kowalik and Murty*, 1993; *Spaulding*, 1994] and even multiple inlets-single bay systems [*Freeman et al*., 1974].

In general, for N number of inlets, we can define

$$K_n=\frac{h_nW_ng}{L_n\left(\frac{r_n}{h_n}+i\omega\right)} \text{ for } n=1,\ldots,N$$

and the resulting expression is

$$\eta_e=\eta_o\left\{\frac{\sum_{n=1}^{N}K_n}{i\omega A_e+\sum_{n=1}^{N}K_n}\right\}$$

In the case of offshore fluctuations of comparable size to the inlet depth, the term K_n can be redefined to take into account the effect of the excess elevation affecting the depth of the inlet:

$$K_n=\frac{(h_n+\eta_o)W_ng}{L_n\left(\frac{r_n}{(h_n+\eta_o)}+i\omega\right)}$$

An approximation to the increased response in frequencies near the natural frequency [*Garrett*, 1972; *Sutherland et al*., 2005] can be estimated as:

$$\Delta\eta_e=\left(1-\frac{\omega}{\omega_n}+\frac{1}{2}i\frac{r}{\omega_n}\right)^{-1}$$

To use the analytical model, an estimate of the linear friction coefficient was necessary. *Scott and Csanady* [1976] used a value of $r=8\times10^{-3}$ m s^{-1} for a location off Long Island at 32 m bottom depth. *Wong and DiLorenzo* [1988] used the same value for their analytical model of two interconnected bays. Meanwhile,

Table 3. Sum of Energy (m^2) in the Different Bands of the Spectra Computed for the Period 2008–2015 Using a 29 Day Hanning Window With Overlapping (50%) Data Segments

Site	Low Frequency	2–5 Days	1–2 Days	Diurnal tide	0.5–1 Days	Semidiurnal Tide	High Frequency
SH	0.023	0.007	0.002	0.008	0.001	0.251	0.002
FBF	0.020	0.007	0.002	0.008	0.001	0.297	0.002
JB	0.020	0.006	0.002	0.008	0.001	0.345	0.004
ERI	0.020	0.006	0.002	0.007	0.001	0.210	0.002
HIC	0.021	0.007	0.002	0.006	0.002	0.230	0.003
PL	0.019	0.006	0.001	0.006	0.001	0.186	0.001
HBF	0.019	0.006	0.002	0.006	0.001	0.175	0.001
LIN	0.019	0.004	0.001	0.001	0.000	0.016	0.001

Lentz et al. [1999] suggest a generic value of $r=10^{-4}$ m s^{-1} for shelf environments with no waves and $r=10^{-3}$ m s^{-1} for conditions with active waves (e.g., surf zone). As inlet linear friction is flow dependent, a value applicable to every environment should not be expected. Instead of choosing a value of friction from the literature and considering that the largest fraction of the flow variability through the inlet is associated with the semidiurnal tide (Table 3), we chose a value of friction for the analytical model to match the transfer of the tides at the M_2 frequency. The ratio between offshore and bay M_2 amplitudes was obtained from the harmonic analysis. We used the analytical model for single-bay systems assuming the connections between adjacent bays were too shallow, long, and narrow (long distance for strong frictional effects to reduce flow) to significantly affect bay response to offshore forcing. Differential phase lag between the contributions of multiple inlets could result in additional uncertainty in the linear friction coefficients.

5. Multibay Analytical Model

The complex bay system of southern Long Island includes a set of interconnected bays with multiple connections to the offshore (Figure 2b). Even the multiple inlets-single bay introduced by *Freeman et al.* [1974] is not sufficient for the southern Long Island inlet-bay complex. An analytical solution can be found for the entire system following the approach in section 4 but with additional expressions for all the connections in the system. The system of equations includes 15 equations and unknowns.

$$\frac{\partial}{\partial t}\begin{pmatrix} u_1 \\ u_2 \\ u_3 \\ u_4 \\ u_5 \\ u_6 \\ u_7 \\ u_8 \\ u_9 \\ u_{10} \end{pmatrix} = g \begin{pmatrix} L_1^{-1} \\ L_2^{-1} \\ L_3^{-1} \\ L_4^{-1} \\ L_5^{-1} \\ L_6^{-1} \\ L_7^{-1} \\ L_8^{-1} \\ L_9^{-1} \\ L_{10}^{-1} \end{pmatrix} \begin{pmatrix} \eta_0-\eta_1 \\ \eta_1-\eta_2 \\ \eta_0-\eta_2 \\ \eta_2-\eta_3 \\ \eta_0-\eta_3 \\ \eta_0-\eta_3 \\ \eta_3-\eta_4 \\ \eta_0-\eta_4 \\ \eta_4-\eta_5 \\ \eta_0-\eta_5 \end{pmatrix} - \begin{pmatrix} u_1 r_1 h_1^{-1} \\ u_2 r_2 h_2^{-1} \\ u_3 r_3 h_3^{-1} \\ u_4 r_4 h_4^{-1} \\ u_5 r_5 h_5^{-1} \\ u_6 r_6 h_6^{-1} \\ u_7 r_7 h_7^{-1} \\ u_8 r_8 h_8^{-1} \\ u_9 r_9 h_9^{-1} \\ u_{10} r_{10} h_{10}^{-1} \end{pmatrix}$$

$$\begin{pmatrix} A_1 \\ A_2 \\ A_3 \\ A_4 \\ A_5 \end{pmatrix} \frac{\partial}{\partial t} \begin{pmatrix} \eta_1 \\ \eta_2 \\ \eta_3 \\ \eta_4 \\ \eta_5 \end{pmatrix} = \begin{pmatrix} h_1 W_1 u_1 - h_2 W_2 u_2 \\ h_2 W_2 u_2 + h_3 W_3 u_3 - h_4 W_4 u_4 \\ h_4 W_4 u_4 + h_5 W_5 u_5 + h_6 W_6 u_6 - h_7 W_7 u_7 \\ h_7 W_7 u_7 + h_8 W_8 u_8 - h_9 W_9 u_9 \\ h_9 W_9 u_9 + h_{10} W_{10} u_{10} \end{pmatrix}$$

If we assume $\eta = \eta e^{i\omega t}$ and $u = ue^{i\omega t}$, then we can define $K_n = \frac{h_n W_n g}{L_n\left(\frac{r_n}{h_n} + i\omega\right)}$ for n = 1,. . .,10,

then with the proper rearrangement, it yields:

$$\eta_3 = \frac{K_5 + K_6 + K_4\left(\frac{K_3\eta_o + \frac{K_1K_2\eta_o}{i\omega A_1 + K_1 + K_2}}{i\omega A_2 + K_2 + K_3 + K_4 - \frac{K_2K_2}{i\omega A_1 + K_1 + K_2}}\right) + K_7\left(\frac{K_8\eta_o + \frac{K_9K_{10}\eta_o}{i\omega A_5 + K_9 + K_{10}}}{i\omega A_4 + K_7 + K_8 + K_9 - \frac{K_9K_9}{i\omega A_5 + K_9 + K_{10}}}\right)}{i\omega A_3 + K_4 + K_5 + K_6 + K_7 \; - \; \frac{K_4K_4}{i\omega A_2 + K_2 + K_3 + K_4 - \frac{K_2K_2}{i\omega A_1 + K_1 + K_2}} \; - \; \frac{K_7K_7}{i\omega A_4 + K_7 + K_8 + K_9 - \frac{K_9K_9}{i\omega A_5 + K_9 + K_{10}}}}$$

The solution for the water level of the central bay can be use to recursively calculate the solutions for the rest of the bays:

$$\eta_2 = \frac{K_3\eta_o + K_4\eta_3 + \frac{K_2K_1\eta_o}{i\omega A_1 + K_1 + K_2}}{i\omega A_2 + K_2 + K_3 + K_4 - \frac{K_2K_2}{i\omega A_1 + K_1 + K_2}}$$

$$\eta_4 = \frac{K_8\eta_o + K_7\eta_3 + \frac{K_9K_{10}\eta_o}{i\omega A_5 + K_9 + K_{10}}}{i\omega A_4 + K_7 + K_8 + K_9 - \frac{K_9K_9}{i\omega A_5 + K_9 + K_{10}}}$$

$$\eta_1 = \frac{K_1\eta_o + K_2\eta_2}{i\omega A_1 + K_1 + K_2}$$

$$\eta_5 = \frac{K_{10}\eta_o + K_9\eta_4}{i\omega A_5 + K_9 + K_{10}}$$

The resulting expressions include all the inter-bay and offshore exchanges. The same limitations of the two-inlet model remain in this solution (e.g., lack of local influences, no overtopping assumed), but it provides a first-order approximation to bay water level transfer.

6. Results

The water level spectra (Figure 3 and Table 3) for all sites exhibited peak energy associated with the M_2 semidiurnal tidal constituent. The remaining frequencies with large spectral energy were the other semidiurnal tidal frequencies (S_2 and N_2), the diurnal frequencies (O_1 and K_1), the storm band (periods between 2 and 5 days), and the low-frequency band (Table 3). The energy in the remaining bands exhibited average fluctuations less than 0.01 m in size.

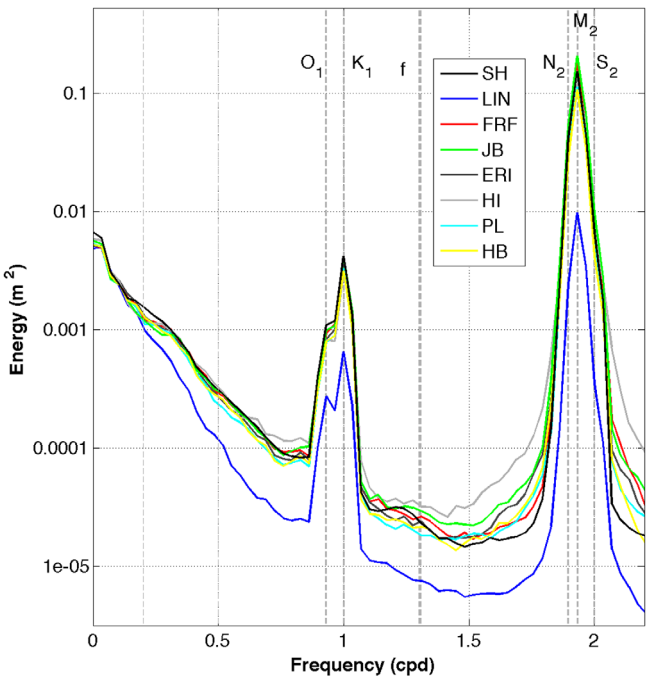

Figure 3. Energy spectra at all stations computed using a Hanning 29 day window with overlapping (50%) data segments. O_1, K_1, N_2, M_2, and S_2 label the principal tidal frequencies and *f* the inertial frequency. (cpd: cycles per day). See Table 1 for key to station abbreviations.

6.1. Great South Bay

The water level dynamics in GSB are investigated using the water level observations at Lindenhurst (LIN). However, in such a sizeable bay, amplitude and phase changes are expected in different areas of the system caused by the local balance between pressure gradient force, surface wind stress, and bottom friction. Analysis of the spatial pattern of water level requires model simulations and additional water level observations.

While storms strongly contribute to the extreme elevation events, tides remain the main source of variability (Figure 3) to the water level in GSB (over 50% of the variance at LIN is

Table 4. M_2 Tidal Amplitude (m) for Each Year 2008–2015[a]

	2008	2009	2010	2011	2012	2013	2014	2015
SH (0.005)	0.681	0.684	0.679	0.683	0.682	0.678	0.678	0.671
FBF (0.005)	0.735	0.740	0.732	0.740	0.737	0.732	0.729	0.724
JB (0.006)	0.791	0.796	0.787	0.797	0.793	0.787	0.785	0.780
ERI (0.003)	0.618	0.622	0.616	0.619	0.620	0.618	0.620	0.615
HIC (0.004)	N/A	N/A	N/A	0.638	0.639	0.636	0.637	0.633
PL (0.004)	0.591	0.594	0.581	0.586	0.581	0.572	0.576	0.563
HBF (0.004)	0.570	0.575	0.561	0.565	0.561	0.560	0.565	0.561
LIN (0.002)	0.175	0.173	0.170	0.167	0.161	0.172	0.186	0.181

[a]Each "year" starts 1 November the previous year and endsE 30 October of the named year; this provides estimates before and after Hurricane Sandy which occurred October 30, 2012. Uncertainty estimates (m) from T_Tide [*Pawlowicz et al*., 2002] are included in parenthesis under the station name.

explained by the tides). The tidal influence in GSB was much smaller than offshore (tides are about 90% of the variance at SH). Water level energy at LIN (Figure 3) was smaller than at SH or at any of the other stations considered for all frequencies except long periods (greater than 10 days). The predominant tidal component at Lindenhurst is the M_2 with yearly amplitudes ranging 0.16–0.19 m (Table 4). The yearly M_2 amplitude at LIN was at an 8 year maximum in 2014 and at a minimum in 2012 (Table 4). The M_2 amplitude for 2013 was not significantly different than the average of the previous years 2008–2012 (consistent with *Aretxabaleta et al*. [2014]), whereas the amplitude for 2014 (November 2013 to October 2014) was significantly larger than previous years ($P = 0.05$).

A monthly time series of M_2 amplitude (Figure 4a) showed a decrease in magnitude after a peak in May 2008 until reaching a minimum in January 2012. The amplitude remained stable during 2012 with a slight decrease after Hurricane Sandy (December 2012). There was an increase in magnitude starting in February 2013 (3 months after Hurricane Sandy) with a peak (0.195 m) in May 2014 and a decrease in magnitude since then. The maximum monthly amplitude change (0.01 m) occurred between March and April 2014. The second largest monthly increase occurred between January and March 2013. The amplitude of the M_2 was at an 8 year minimum in 2012 (Table 4). The monthly minimum occurred 2 months after the passage of Hurricane Irene (August 2011). The change in monthly M_2 amplitude was approximately 5% of the total monthly average.

The amplitude of the next largest tidal constituent, K_1 (Figure 4d), was much smaller ($\sim$0.04 m) than the M_2 and the RMS monthly variability was 0.005 m. The amplitude of the other main diurnal constituent, O_1 (Figure 4e), was less than 0.03 m. The next largest constituent, N_2 (Figure 4b), with average amplitudes slightly larger than 0.03 m, had much smaller fluctuations than the other semidiurnal constituents included. Finally, the amplitude of the S_2 semidiurnal tide (Figure 4c) was also slightly less than 0.03 m. The percentage changes of tidal amplitude for the remaining constituents considered were much larger (around 10–15%) than the M_2 changes in relation to their respective average value. The correlation between the fluctuations of M_2 amplitude and the other constituents were less than 0.2 (not significant).

The monthly estimates of M_2 phase at LIN oscillated between 68° and 75° (3.5° uncertainty). Peaks in phase (increased lag) occurred 1–3 months after the hurricanes (4° increase after Irene and 2° after Sandy). However, the phases returned to average values after 2–3 months. Although small changes in phase lag after the two hurricane events were observed, there were changes of similar magnitude during nonstorm periods. The S_2, N_2, and K_1 tidal constituents had larger phase fluctuations but the errors in phase calculations were also much larger than the M_2 phase.

The overtides and compound tides of the principal tidal constituents may be significant in some areas where nonlinearities dominate. The amplitude of the M_4 (0.018 m) and M_6 (0.012 m) tidal constituents at Lindenhurst were of a similar magnitude as at SH (0.015 and 0.016 m, respectively), but they are expected to be more sizeable in the proximity of Fire Island Inlet (no data available). The similar sizes of the overtides offshore and in the Bay suggest that the nonlinear frictional effects on the tide were only about 10% in the Bay and less than 2% in the ocean. The small overtides suggest that the linear drag coefficient in the inlet and bay used in the simple analytical model was appropriate, as nonlinear frictional effects might result in a much larger increase in the size of the overtides.

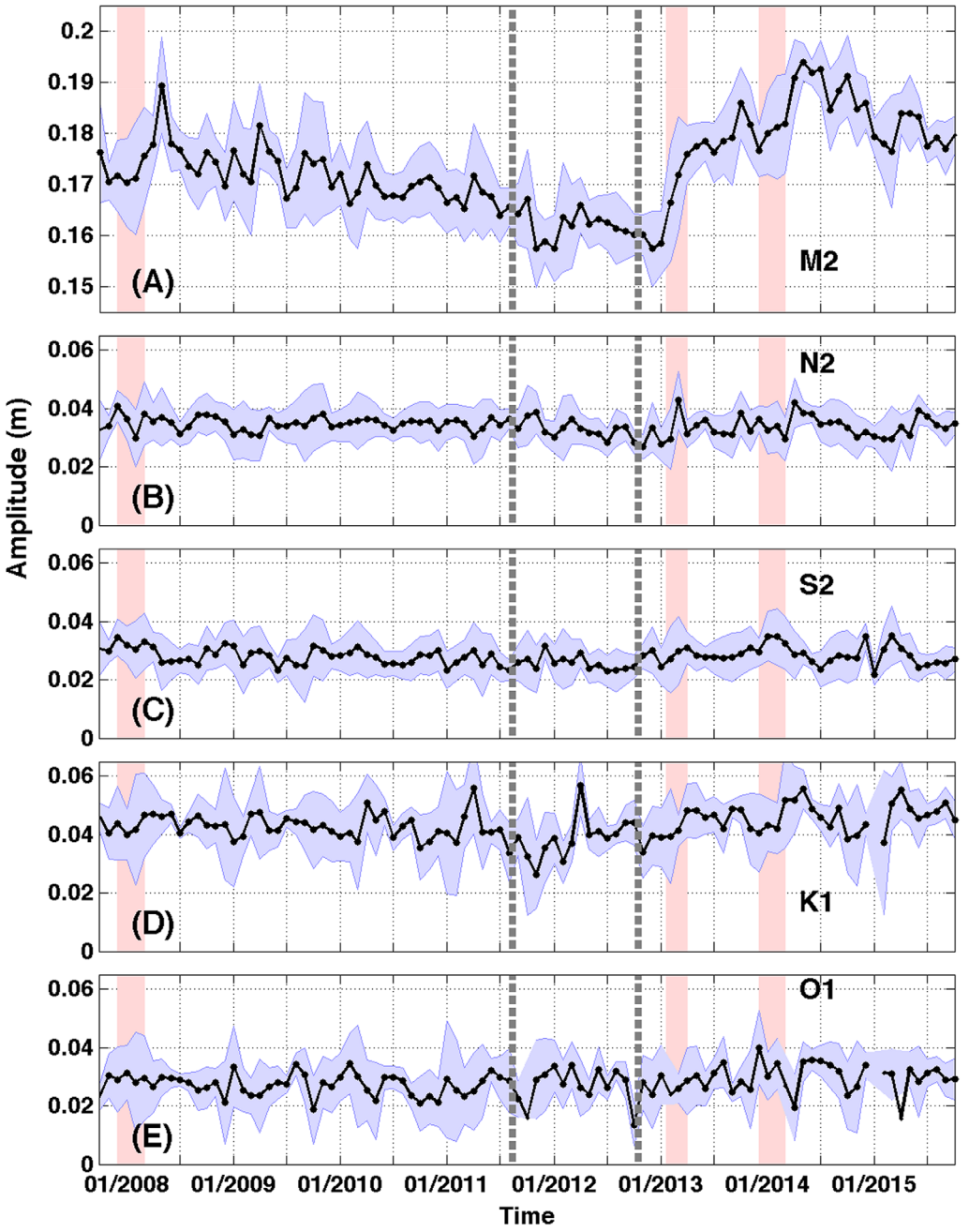

Figure 4. Monthly tidal amplitude (m) at Lindenhurst (LIN) for the five main tidal constituents. Envelope (light blue) are T_tide error estimates. The vertical dashed lines indicate the occurrence of Hurricanes Irene (August 2011) and Sandy (October 2012). The vertical shaded areas indicate the times of dredging at or around Fire Island Inlet. Note that the vertical scale for the M_2 amplitude panel is different than for the other panels and it does not include 0 m.

The transfer function (Figure 5) between Sandy Hook (SH) and Lindenhurst (LIN) showed small changes in the 5 years of data considered (two before and three after Hurricane Sandy). The transfer curves were consistent with the previous analysis of *Aretxabaleta et al.* [2014]. The transfer of the offshore fluctuations was 60–80% at periods between 2 and 10 days, about 40–50% at diurnal periods, and about 20–30% at semidiurnal periods. While the transfer for 2011 (November 2010 to October 2011) and 2013 (November 2012 to October 2013) were quite similar, the values for 2012 (year before Hurricane Sandy) were lower for tidal and subtidal frequencies. The transfers for 2014 (November 2013 to October 2014) were higher than other years at most frequencies. The values for 2015 (November 2014 to October 2015) were smaller and represented a

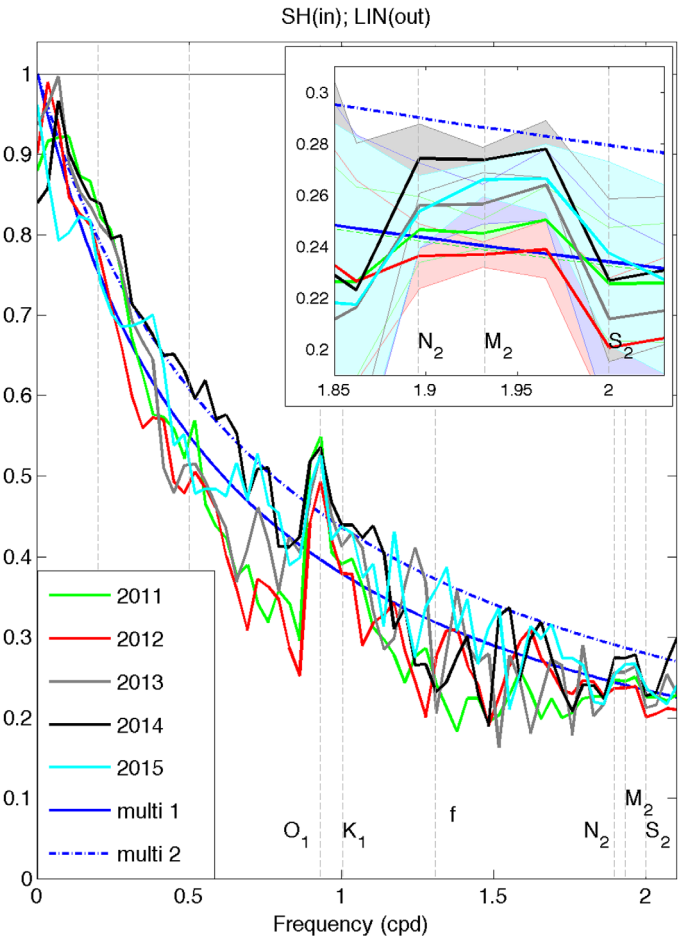

Figure 5. Transfer function between Sandy Hook (SH) and Lindenhurst (LIN) for 5 years (each "year" starts in November the previous year, so for instance, the 2012 curve includes data from November 2011 to October 2012). The solid blue line is the analytical model from this study with a single-opening representing Fire Island Inlet (linear friction r = 0.017 m s^{-1}). The dashed-dotted blue line includes the analytical model with both Fire Island Inlet (r = 0.017 m s^{-1}) and the Wilderness Breach (r = 0.034 m s^{-1}). The inset is a zoom in the semidiurnal frequencies and includes the uncertainty envelopes [*Bendat and Piersol*, 1986] of each yearly transfer estimate.

partial return to the pre-2014 conditions. The transfer function at the M_2 frequency for 2014 was outside the uncertainty envelope for the long-term mean but still within the envelope for 2015. The water level transfer in the storm band (2–5 days) during the period between Hurricane Irene and Hurricane Sandy (2012) was significantly smaller (outside the uncertainty envelope) than during any of the other years. The remaining differences between years were within the uncertainty envelope using the *Bendat and Piersol* [1986] formulation at most frequencies, suggesting that while differences existed they are not significant.

The bimonthly percentage change in transfer function for 2008–2015 (Figure 6) demonstrates that the bay response was generally stable at all frequencies with relatively small magnitude fluctuations. The changes at frequencies less than 0.5 day^{-1} were quite noisy as the spectral estimates for subsets of bimonthly intervals contained limited observations. The period between Hurricanes Irene and Sandy was characterized by smaller transfer coefficients at most frequencies especially the semidiurnal tides and, immediately after Irene, the storm band (2–5 days). The enhanced transfers at semidiurnal frequencies after Hurricane Sandy were most evident during the period February 2014 to September 2014 and represented a 5–15% increase in transfer. Semidiurnal transfer values were mostly within 5% of average by the end of the record (October 2015). The diurnal tidal frequencies showed increases in both early 2014 and 2015, returning to average values after a few months. The timing and relative magnitude of the percentage changes in the tidal bands (Figure 6) were consistent with the changes described in the harmonic analysis (Figure 4). The transfers in the storm band peaked around October 2014 and sharply decreased after then.

The analytical model (section 4) was fit (in a least square best fit) to obtain a linear friction coefficient for the period before Hurricane Sandy (October 2007 to October 2012) when only the Fire Island Inlet was open and prior to the dredging in 2013 and 2014. The resulting coefficient was r = 0.017 m s^{-1} and the associated frictional adjustment time was around 5–10 min. The analytical curve (Figure 5) matched the transfer function shape for most frequencies, consistent with the transfer being dominated by the size of the inlet and area of the bay and not by the size of the fluctuations at a specific frequency. The analytical curve overestimated the transfer for periods between 1 and 2 days (water level energy less than 10^{-4} m^2 in that band) and underestimated the fluctuations around the O_1 tidal frequencies, while matching the K_1 tide. The mismatch at the O_1 frequency might be associated with additional effects inside the bay that contribute to enhanced diurnal oscillations. The natural frequency of the Bay was 0.5 h^{-1} and did not affect the frequencies considered in this study.

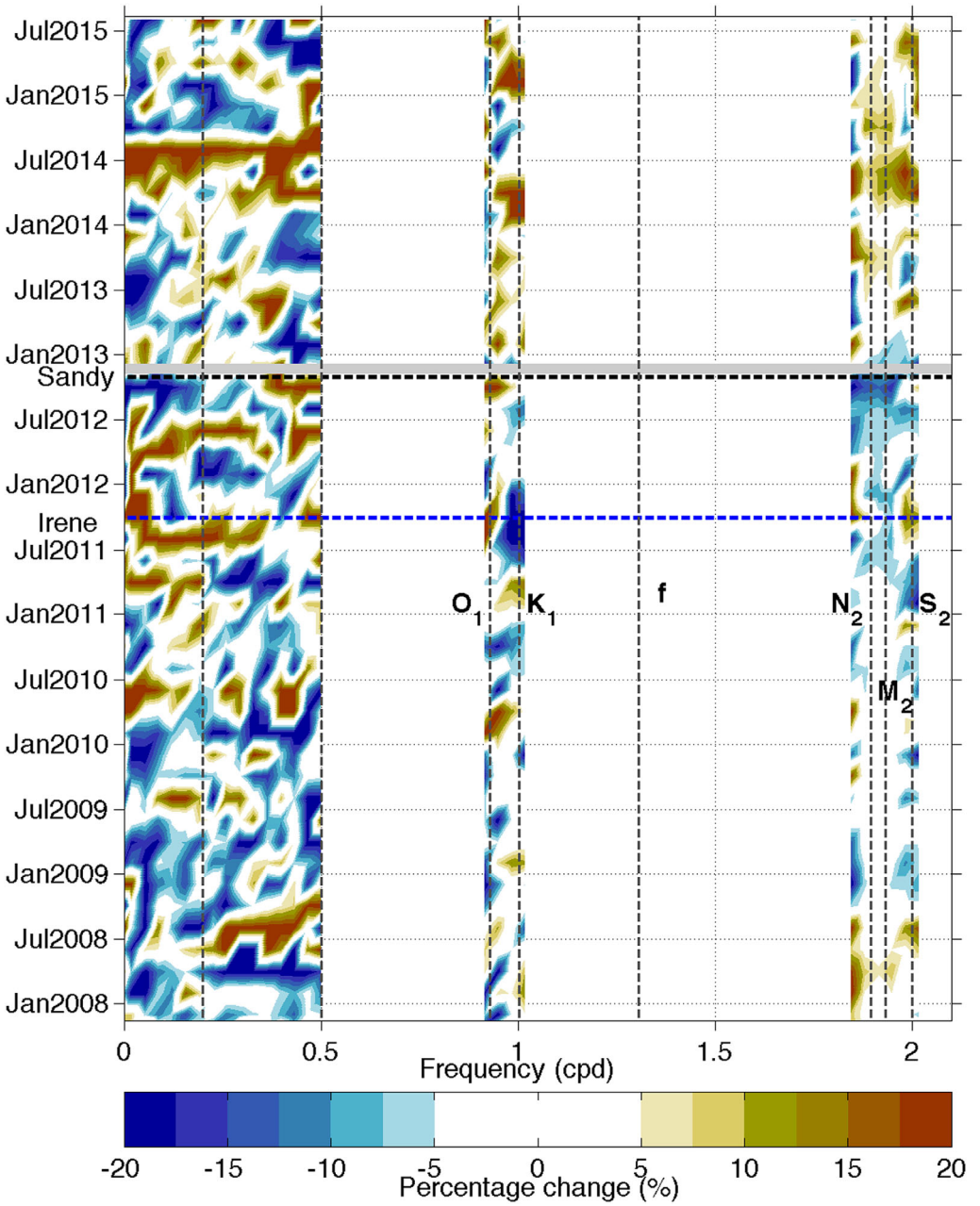

Figure 6. Bimonthly percentage change from average (at each frequency) transfer function (for the period 2008–2015) between Sandy Hook (SH) and Lindenhurst (LIN). Only the frequencies with energy values at LIN above 10^{-4} m^2 (equivalent to fluctuations larger than 0.01 m) are included. The timing of Hurricanes Irene (blue dashed line) and Sandy (horizontal black dashed line) and the associated missing data are indicated.

When the dimensions of the Wilderness Breach for June 2014 (600 m^2 cross-sectional area, http://po.msrc.sunysb.edu/GSB/) were added to the analytical model using two inlets and the 2007–2012 friction coefficient for both inlets, the theoretical curve matched the 2014 transfer function for subtidal frequencies, improved the match at the diurnal frequencies, but slightly overestimated the transfer of the semidiurnal tides by 0.01. A larger friction coefficient (0.034 m s^{-1}) at the Wilderness Breach was needed to match the semidiurnal tide magnitude with the analytical model. However, matching the M_2 tide resulted in a slight underestimation of the response in the storm band. If the smaller Wilderness Breach cross section from the period immediately following Sandy (or after 2015) was used (~400 m^2 cross-sectional area), then the needed frictional enhancement was smaller.

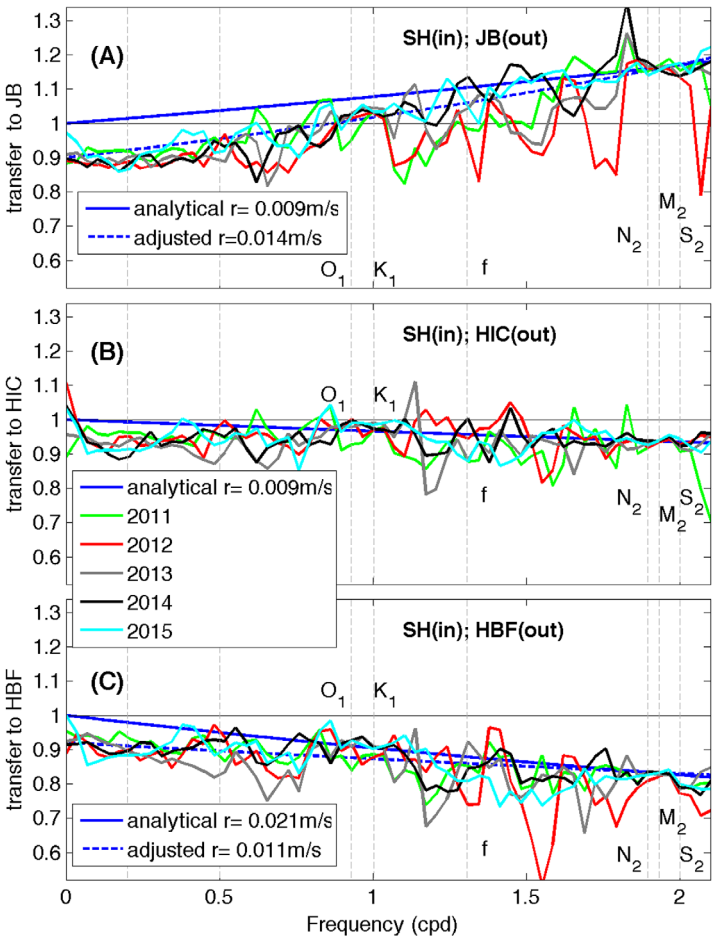

Figure 7. Transfer function between Sandy Hook (SH) and (a) Jamaica Bay (JB), (b) Hog Island Channel (HIC), and (c) Hudson Bay at Freeport (HBF) for 5 years (each "year" starts in November the previous year, so for instance, the 2012 curve includes data from November 2011 to October 2012). The solid blue line is the analytical model (section 4) with one single opening and a linear friction coefficient matching the M_2 transfer for the average of all years for (a) Rockaway Inlet, (b) East Rockaway Inlet, and (c) Jones Inlet. The dashed blue line represents the analytical model adjusted to match the transfer at zero and M_2 frequencies.

6.2. Jamaica Bay

The water level energy in Jamaica Bay (JB, Table 3), both at the eastern end of the Bay (JB station) and at the Rockaway Inlet entrance (FBF station), was smaller than at SH for long periods, slightly smaller in the storm band, and larger than SH at the diurnal and especially semidiurnal bands (~30% enhancement between SH and JB). The tidal fluctuations at the JB station exceeded the offshore values and explained 93% of the Bay water level variance. The amplitude of the main tidal constituent, M_2, was 0.79 m with less than 1% (not significant) interannual differences (Table 4). The M_2 was enhanced around 8% between offshore and the inlet (FRF) and about 16% between offshore and the Bay. The other main components of the tide at JB were N_2 (0.18 m), S_2 (0.15 m), K_1 (0.11 m), and O_1 (0.05 m). The ratio of the semidiurnal tides to the diurnal amplitudes was intensified compared to offshore conditions. There was no relationship between monthly variations in tidal amplitude and the timing of Hurricane Sandy or any other large storm. The overtides at FBF were around the same size as at SH suggesting small nonlinear contributions. Inside the Bay, the overtides were enhanced from values at SH by 60–80%. (M_4, 0.027 m; M_6, 0.027 m). The natural frequency of Jamaica Bay was about 2 h^{-1} and thus not a factor at the frequencies considered in this study.

The response of Jamaica Bay to offshore forcing was investigated with the transfer function between SH and JB (Figure 7a) and between SH and FBF. The transfer function between SH and FBF was close to unity (not shown), consistent with minor attenuation between the ocean proxy and the bay entrance. Bay water levels at JB were greater than offshore at most frequencies larger than 1 day^{-1}. The Rockaway Inlet channel is deeper than 10 m in many areas and thus frictional effects that reduce water exchange are small. The transfer values for periods between about 2 and 15 days were around 90% and fairly constant. The transfer for periods shorter than 45 h exceeded unity for diurnal and semidiurnal frequencies. The high-frequency transfers were enhanced inside Jamaica Bay and the small frictional effect was not sufficient to attenuate the oscillations. There was small interannual variability in the transfer function to JB with no significant change associated with any of the large storm events (hurricanes).

The analytical model (Figure 7a), using a linear drag coefficient to provide a best least squares fit at the semidiurnal tidal transfer for all years ($r = 0.009$ m s^{-1}), overestimated the transfer at most other frequencies. The primary mismatch in the predicted transfer was at low frequencies, where the model

predicted a full transfer of water level at zero frequency, as offshore fluctuations would have infinite time to enter the bay. The observations suggested only around 90% of the low-frequency offshore fluctuations were present at JB. The analytical model was adjusted to provide the best fit in the least squares sense to the observed transfer at zero and M_2 frequencies. The resulting linear drag coefficient was $r = 0.014$ m s^{-1}. The predicted transfer function more closely matched the 90% transfer at low frequencies, and continued to closely match at M_2 (95% of the energy). The linear friction for the adjusted model was close to the value for GSB and was likely more realistic. The resulting model approximated the observed diurnal transfer and only slightly overestimated transfer in the storm band. The skill of the analytical model is limited by the assumption that the bay water level is controlled by inlet friction. In Jamaica Bay, water level, especially the semidiurnal tide, behaves more like a reflected cooscillation between offshore and bay.

6.3. East Rockaway Inlet Bay System

The East Rockaway Inlet bay system includes the areas directly affected by the flow through East Rockaway Inlet (ERI). The inlet is directly connected with the narrow (~200 m) and long (~5000 m) Reynolds Channel. The length and width of the channel might suggest strong frictional effects, but these geometric constraints are compensated by the small area of the adjacent bay system.

The dominant tidal amplitude at Hog Island Channel (HIC) was the M_2 with values around 0.64 m and small interannual changes (Table 4). The maximum annual amplitude of the M_2 constituent at HIC was in 2012, but the monthly maximum was in June 2014, the same time as the maximum observed at LIN. While the overtides were small (M_4, 0.003 m; M_6, 0.015 m) in the proximity of the inlet at ERI, they were slightly enhanced (M_4, 0.016 m; M_6, 0.024 m) in the interior of the Bay.

The transfer function between SH and HIC (Figure 7b) was close to unity (between 0.9 and 1) for all frequencies. There were some interannual differences but mostly in frequencies with limited energy (Table 3) and high uncertainties (low coherence between the time series). While transfer of the diurnal tides exhibited some interannual changes (smaller O_1 transfer during 2011), the transfers at semidiurnal frequencies for all years were similar in magnitude. There was a slight (not significant) transfer enhancement in periods around 18–21 h, but the energy in that band was small (0.002 m^2, Table 3) and the uncertainty quite high (up to 30% in that band). About half of the attenuation between SH and HIC occurred between the East Rockaway Inlet (ERI) station and HIC.

The analytical model (Figure 7b) overestimated the transfer at low frequencies (periods larger than 2 days), while slightly under predicting the diurnal transfer values. The long Reynolds Channel caused a minimum change in transfer across the spectrum and resulted in low linear friction estimates for the analytical model ($r = 0.009$ m s^{-1}).

6.4. Jones Inlet Bay System

The bay system to the west of Great South Bay includes the areas directly affected by the flow through Jones Inlet. The dominant tidal amplitude at Hudson Bay at Freeport (HBF) was the M_2 with values around 0.56 m and interannual changes on the order of 4% (Table 4). The largest yearly M_2 amplitudes (Table 4) occurred in 2008–2009 after the dredging of Jones Inlet in 2008. The monthly time series of M_2 amplitude (Figure 8a) showed fairly constant values (0.55–0.58 m) after Hurricane Sandy with a sudden increase in May 2014 (peak of 0.58 m). The maximum monthly amplitude change (0.02 m) occurred in April 2014, the same time as the M_2 amplitude change at LIN. The minima in M_2 amplitude (0.54 m) were observed in September 2010 and December 2011. The monthly peak in May 2014 (over 0.58 m) occurred after the spring 2014 Jones Inlet dredging. The monthly changes in the amplitude of the N_2, S_2, K_1, and O_1 tidal constituents (Figure 8) were of the same size as the M_2 changes, but much larger in proportion to their respective average amplitudes.

The transfer function between SH and HBF (Figure 7c) was between 75 and 95% for all frequencies (except in some bands of very low energy). Most of the reduction in transfer occurred between SH and Point Lookout (PL) as the transfer between PL and HBF was close to unity except for a 5% reduction of the semidiurnal tides. The transfers in the storm band were between 80 and 95% with higher values during 2011 and 2014. For the diurnal tides, the O_1 transfer was smaller during 2011 than any other year (as in HIC). The transfer at the M_2 frequency was slightly smaller during 2012 (change was around 1%), which was consistent with the

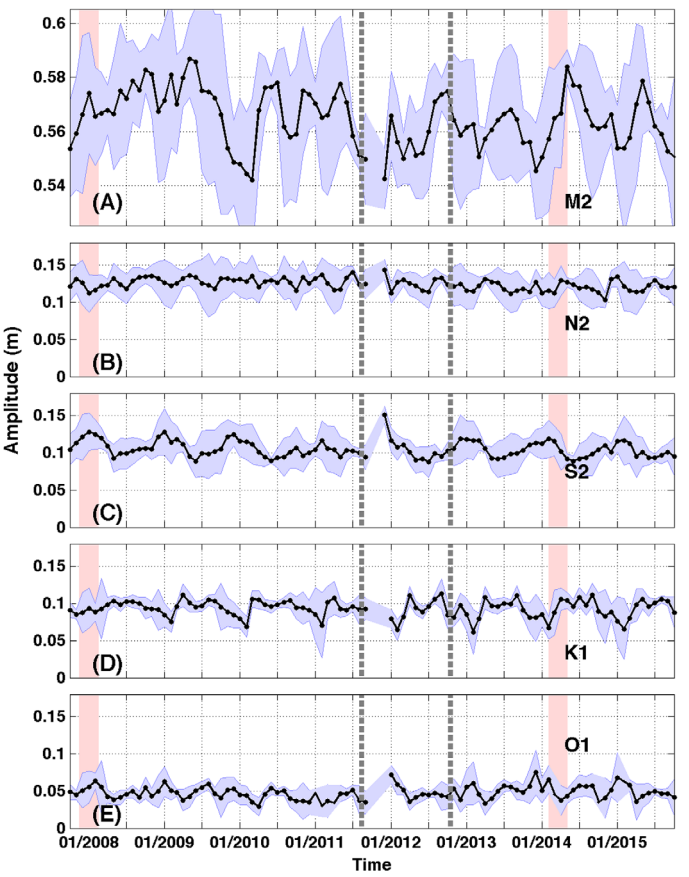

Figure 8. Monthly tidal amplitude (m) at Hudson Bay at Freeport (HBF) for the five main tidal constituents. T_tide error estimates are provided in light blue. The vertical dashed lines indicate the timing of Hurricanes Irene (August 2011) and Sandy (October 2012). The vertical shaded areas indicate the times of dredging at Jones Inlet. Note that the scale for the M_2 amplitude panel is different than for the other panels.

M_2 amplitudes from the harmonic analysis (Figure 8a). The interannual changes in the other semidiurnal frequencies were smaller than 5% and with no clear temporal pattern.

The analytical model (Figure 7c) with a friction coefficient that provided the best fit in the least squares sense of the transfer of the M_2 tide (linear friction of 0.02 m s^{-1}) overestimated the transfer at periods longer than 2 days, but reproduced the diurnal transfer (similar to Jamaica Bay). The observations suggested that between 90% and 95% of the near-zero frequency offshore fluctuations were present at HBF. If the analytical model was adjusted (r = 0.011 m s^{-1}) to provide a best fit of the observed transfer at zero and M_2 frequencies (95% of the energy), the resulting transfer approximated the observed storm band transfer but underestimated the diurnal tidal transfer.

6.5. All Connected Bay Systems

A formulation that considered all the inlets and channels between connected bays (all except Jamaica Bay) in the southern Long Island bay system was developed (section 5). The multibay formulation permitted the simultaneous calculation of water level transfer for all bays and also allowed for the estimation of the transfer in both Shinnecock and Moriches Bay, where observations were not available.

The results of the multibay formulation (Figure 9) were consistent with the transfers described in the previous section. The analytical model captured the diurnal and semidiurnal transfers at HIC and HBF and showed skill in the tidal transfers at LIN (with the exception of the enhanced O_1 transfer as described previously). It slightly overestimated the transfer in subtidal frequencies at LIN and overpredicted the subtidal response at HIC and HBF (because of the observed transfer at very low frequencies not matching unity as predicted in the theory). The friction coefficient was 0.016 m s^{-1} for all connected bays except an enhanced friction of 0.035 m s^{-1} for the Wilderness Breach.

The modeled transfer response in Moriches Bay was around 55% at semidiurnal frequencies (consistent with offshore/bay tidal gradients from *U.S. Army Corps of Engineers*, [2001]), between 65 and 70% at diurnal frequencies, and 80–90% at storm frequencies. In the case of Shinnecock Bay, the estimated transfer coefficients were slightly higher with 90–95% transfer at storm frequencies, approximately 70% transfer at semidiurnal frequencies (*U.S. Army Corps of Engineers* [2001] provided tidal differences between offshore and bays corresponding to 70–75%), and 80–85% transfer at the diurnal frequencies. These values were sensitive to the choice of linear friction used for the analytical model. If the offshore to bay semidiurnal tidal amplitude ratio from offshore to Moriches and Shinnecock Bays from *U.S. Army Corps of Engineers* [2001] was used to estimate the friction coefficient at Moriches Inlet and Shinnecock Inlet, the resulting friction was 0.014 m s^{-1} at Moriches Inlet and 0.013 m s^{-1} at Shinnecock Inlet.

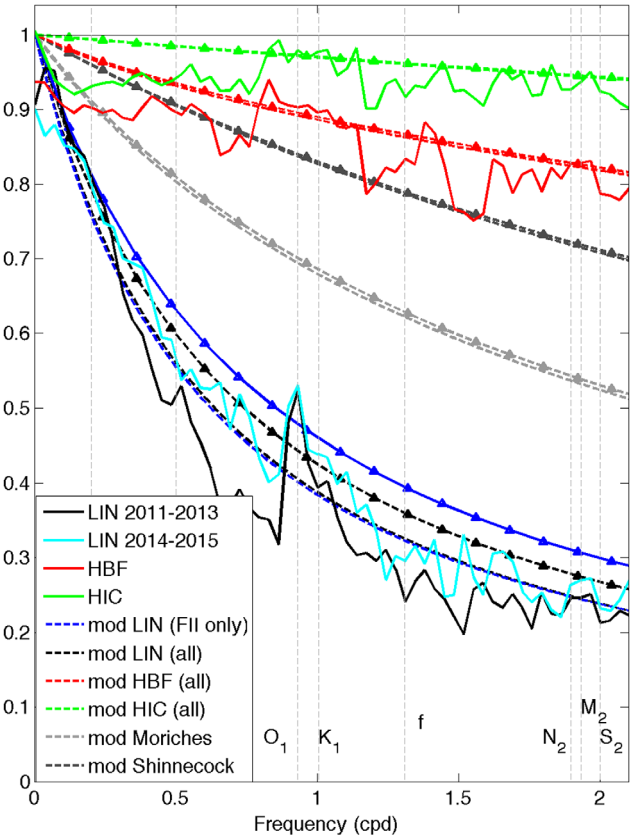

Figure 9. Analytical model estimates of the transfer function (section 5) for all bays including Moriches Bay and Shinnecock Bay (long-term observations to support analytical estimates for Moriches and Shinnecock Bays were not available, but *U.S. Army Corps of Engineers* [2001] were used as a skill metric). Transfer estimates from the analytical model are shown under two different scenarios: with no Wilderness Breach (dashed lines) and with an open Wilderness Breach (triangle markers). The difference between open and close breach estimates was small in most bays and the curves overlap. The exception was Great South Bay (LIN). The observed transfer at LIN, HBF, and HIC is included for comparison (solid lines).

When the Wilderness Breach was considered as an additional connection with the offshore, the transfer enhancement was limited to Great South Bay (approximately 10% increase in magnitude from no-breach case) with negligible effects (less than 1% change in magnitude) in Moriches Bay and the Jones Inlet Bay system. To match the tidal enhancement at Lindenhurst (2014–2015 average), the friction in the analytical model that included the breach needed to be adjusted by around 10%. If instead of modifying the friction, the dimensions of Fire Island Inlet were altered, a similar effect was achieved.

7. Discussion

7.1. Relationship Between Water Level and Geomorphic Changes

A key question is whether observed changes in M_2 amplitude (Figures 4 and 8) could be attributed to morphological changes caused by intense storms (hurricanes) or to dredging of the Great South Bay system. The strength of the M_2 amplitude at LIN (Figure 4) ranged from 0.16 m to about 0.19 m over the period 2008–2015. Increases in M_2 at LIN of about 0.01 m in April 2008 and April 2014 followed dredging of Fire Island Inlet and Jones Inlet. An increase of about 0.02 m in February to March 2013 occurred following dredging of Fire Island Inlet, and a simultaneous increase in the cross section of the Wilderness Breach by a factor of 3–4 (from around 100 m^2 in December 2012 to almost 300 m^2 in February 2013 and over 400 m^2 in March 2013, http://po.msrc.sunysb.edu/GSB/). Nearly identical minimum M_2 amplitudes (0.157 m) over the period 2008–2015 followed Hurricanes Irene and Sandy by about 1 month. Decreases in tidal amplitude occurred after major storm activity (–0.01 m in September 2011 after Hurricane Irene; −0.003 m in December 2012 after Hurricane Sandy). The correlation between M_2 amplitudes at LIN and Wilderness Breach cross-section area after December 2012 (15 observations) was $R^2 = 0.81$ ($P < 10^{-5}$). There was no clear change in the N_2, S_2, K_1, or O_1 constituents at LIN associated with the M_2 events; however, the amplitude of the diurnal (K_1, O_1) and the other semidiurnal (N_2 and S_2) amplitudes was less than 0.04 m (±0.01 m), making it difficult to identify changes smaller than 0.01 m. The correlation between the amplitudes of N_2, S_2, K_1, and O_1 constituents and the breach cross section was between 0.05 and 0.3. One of the minima in M_2 amplitude at HBF also occurred during the period between Hurricanes Irene and Sandy. The increase in M_2 amplitude at HBF in early 2008 occurred at the time of a dredging project in Jones Inlet. The monthly amplitude peak at HBF in May 2014 occurred after the spring 2014 Jones Inlet dredging. The correlation between M_2 amplitudes at HBF and Wilderness Breach cross-section area was $R^2 = 0.24$ ($P = 0.06$).

The timing of the dredging projects appears to be associated with an increase in the amplitude of the dominant tidal component (M_2). The largest changes in the M_2 at LIN and HBF were observed in the 1–2 months after dredging was reported in Jones Inlet and Fire Island Inlet. The effect of dredging subsides after periods

between a few months and a year. Fluctuations in the size of the Wilderness Breach also appear to have affected the increase in M_2 amplitude in Great South Bay after Hurricane Sandy (high correlations), but they cannot explain the changes at LIN before the opening of the inlet or the changes at HBF. While we are able to evaluate the effects of dredging at times when no breach is present, to separate the contribution of the changing breach size we would need a case when a breach was present without any dredging intervention, but such a case was not available in the observed record.

The combined impacts of Hurricanes Irene and Sandy caused erosion of the modern sediment deposit on the inner shelf offshore of Fire Island, with sediment transported in a general southwesterly direction [*Schwab et al*., 2013, 2016]. Surveys of the shoreface and subaerial components of Fire Island indicate that the eroded sediment was not transferred to the shoreface or adjacent barrier [*Schwab et al*., 2016]. Some of the mobilized sediments were likely deposited in the Fire Island Inlet system in the months following Sandy. The additional sediment would have altered the size and effective depth of the inlet resulting in smaller water level transfer in the months after the Hurricanes Irene and Sandy.

7.2. Independence of Transfer From Fluctuation Amplitude

To evaluate changes in vulnerability due to the size of storm-induced fluctuations, we consider the possibility that water level associated with intense storms might have larger proportional effect (i.e., larger transfers) in the bays than smaller oscillations. *Aretxabaleta et al*. [2014] showed that the daily maximum subtidal water levels for large events recorded during the period 2007–2013 followed the same linear relationship as the subtidal water level of smaller fluctuations. To test the effect of the size of the fluctuations on the transfer response, we separated times with large and small low-frequency fluctuations. Two time series of unfiltered observations were created for LIN: one including times when low-pass filtered data (5 day low-pass filter) exceeded 0.1 m and another for times when the filtered data were below 0.1 m. Time series of unfiltered SH observations were also created for the periods of large and small fluctuations identified in the two LIN series. The transfer between SH and LIN was calculated for both time series using the unfiltered data (Figure 10). The differences in tidal frequencies were negligible (less than 2%). The transfer of small fluctuations was 10–30% smaller in the low-frequency band because the 0.1 m cutoff limited the size of observations in that band. There were also reduced transfers around the inertial band likely as a result of the limited inertial effects in the bay. The uncertainty in the inertial band was also large. In the storm band (2–5 days), the values of transfer of large fluctuations were sometimes higher (up to 10%) and sometimes lower (less than −8%) than the values for small fluctuations. The differences in the storm band averaged 2.5% and were within the uncertainty envelope [*Bendat and Piersol*, 1986]. The analysis highlights the independence of the transfer from the magnitude of the fluctuations at a specific frequency.

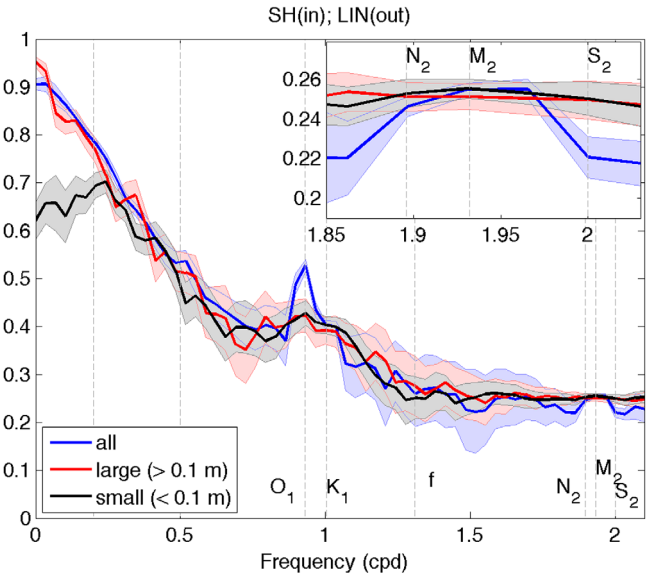

Figure 10. Observed transfer function between Sandy Hook (SH) and Lindenhurst (LIN) for 2008–2015. The data are grouped based on the size of the oscillations: large fluctuations (larger than 0.1 m, energy values at LIN above 10^{-2} m^2) are shown in red; small fluctuations (smaller than 0.1m at LIN) in black; and the combined data in blue.

An underlying assumption for the predictive capability of the model for extreme events is that the physics of the inlet/bay system remain the same even during large fluctuations. During extreme storm events (e.g., 1938 Hurricane, Hurricane Sandy), the conditions in the inlet might be altered (e.g., increased bottom roughness caused by waves, increased inlet depth caused by surge and wave setup) and the barrier island might over top. Some of the effects might be partially offsetting (deeper inlet results in less bottom friction, while waves cause higher friction due to increased roughness). However, these effects could alter bay water level response

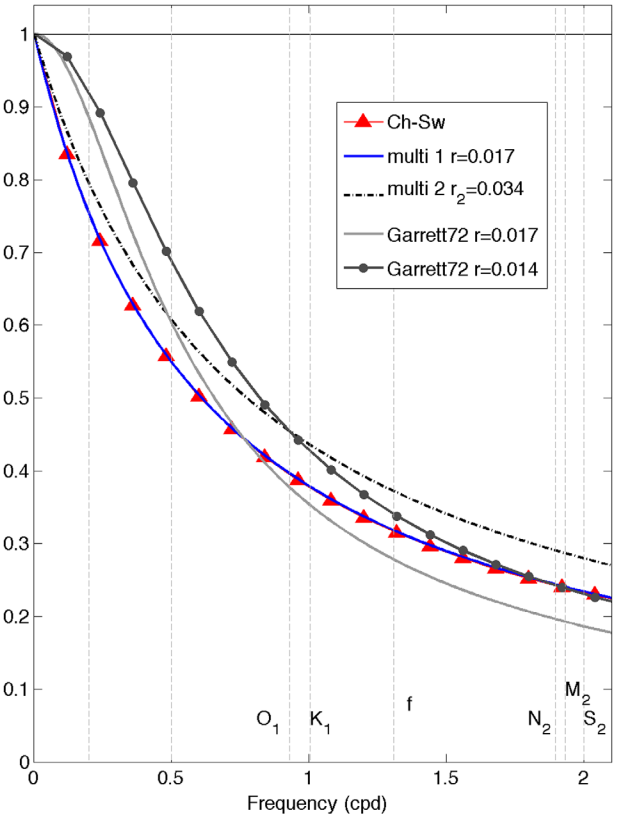

Figure 11. Predictions of sea level transfer coefficient for Great South Bay for various models and friction coefficients. "Ch-Sw" stands for the single inlet *Chuang and Swenson* [1981] model. "Multi 1" uses the model introduced in this study but including a single inlet (Fire Island Inlet). "Multi 2" uses the model introduced in this study but including both Fire Island Inlet and the Wilderness Breach (with double friction at the breach location). Garrett72 uses the *Garrett* [1972] model of a bay in near-resonance with the offshore.

during extreme events from that predicted for the average geometry and friction coefficient. Nevertheless, the estimate of the difference in transfer for large and small events of order 10% suggests that the transfer may not be vastly different, especially if the basic geometry remains unchanged. The analytic model provides a framework to assess the potential magnitude of changes in transfer caused by inlet geometry or friction; changes in bay response could also be addressed with a fully nonlinear three-dimensional hydrodynamic model simulation. The biggest constraint for evaluating transfer during extreme events is the uniqueness of each event and the lack of observations during them.

7.3. Comparison With Alternative Analytical Model

The model proposed in section 4 matched the transfer relationship obtained with the *Chuang and Swenson* [1981] formulation (Figure 11) when only a single inlet was considered. The inclusion of the second inlet to GSB in the analytical model provided information regarding the different frictional character of both inlets (Wilderness Breach was more frictional). Additionally, the analytical model can be compared with other formulations. *Garrett* [1972] proposed a simple model for a bay system in near-resonance connected to the open ocean. The Garrett formulation has been applied to multiple systems (Juan de Fuca Strait [*Sutherland et al.*, 2005]; Bay of Hudson [*Arbic et al.*, 2007]). After some simplifications, the water level "enhancement" can be expressed as $\Delta\eta_e = (cos\left(\frac{1}{4}\frac{\omega}{\omega_n}\right) - \frac{1}{2}i\frac{r_b}{\omega_n}sin\left(\frac{1}{4}\frac{\omega}{\omega_n}\right))^{-1}$ The linear friction parameter, r_b, in this model is the friction that attenuates the near-resonance fluctuation inside the bay rather in the channel. The resulting curve applied to GSB (Figure 11) matched the presented model in the semidiurnal frequencies after minor frictional adjustments (Garrett model required less friction to match semidiurnal transfers), but slightly overestimated the transfer at low frequencies. While both models differ in their representation, they included some common physics and comparable assumptions and thus produced similar results. The similar behavior of the models in GSB could be explained by the fact that most of the bay friction in the Garrett model is likely to occur in the vicinity of the inlet. The Garrett model represents a better approximation to systems where the inlet friction contribution to bay water level dynamics is more limited (e.g., current geometry of Jamaica Bay). A complementary method to address the robustness of the linear approach will be a comparison with a fully nonlinear three-dimensional hydrodynamic model simulation, but such modeling is beyond the scope of this study.

7.4. Analytical Model Application: Factors Controlling Transfer in Jamaica Bay

Over the last several decades, there has been a reduction in marsh and seagrass beds in Jamaica Bay due to human impacts [*NYCDEP*, 2007]. The surface area of the bay has been reduced from 101 km^2 in the mid nineteenth century to 53 km^2, while the volume of the bay has increased 350% [*NYCDEP*, 2007]. Increases in tidal ranges seem to be a consequence of natural and engineering modifications that occurred in the bay during the first half of the twentieth century. *Swanson and Wilson* [2008] proposed that there was a relation between

marsh disappearance and tidal range increase. The analytical model (Section 4) was used to estimate the relative importance of changes in area and water depth on the water level response of the bay. Using conditions valid for the 1800s (approximately double bay area and about half of the inlet depth [*NYCDEP*, 2007]), the model predicted a slight reduction in the bay response (less transfer). The reduction resulted from the combined effect of the larger area and additional friction along the shallower Rockaway Inlet. Under current bay conditions, the increased water depth along the inlet and the maintenance of the navigation channel though periodic dredging resulted in a larger transfer of water level from offshore (close to unity in the storm band). The larger inlet depth and width appear to be the controlling factors that facilitated the exchange with the offshore and might have affected the marsh and seagrass beds in Jamaica Bay. The analytical results are consistent with hydrodynamic modeling simulations of the area [*Orton et al*., 2015] that quantified the effect of narrowing and shallowing Rockaway Inlet. The potential benefit of different restorative approaches (e.g., inlet narrowing and/or shallowing and bay shallowing) are now being explored (http://adaptmap.info/).

7.5. Additional Mechanisms Affecting Water Level in Bays

The most relevant cause of the bulk exchange between the bay and the shelf is the remote forcing by winds and tides. Meanwhile, local wind forcing can dominate the transport and exchange inside the bay. The contribution of local wind acting directly on the surface of the bay also causes current fluctuations and water level setup, especially in large bays. *Wong and Moses-Hall* [1998] found remote effects were more important to the bulk estuary exchange (e.g., water level) in Delaware Bay, while local effects controlled the transport and distribution of materials. In the presence of strong stratification, vertical shear in velocity is expected as a response to local wind stress [*Garvine*, 1985; *Wong and Moses-Hall*, 1998; *Janzen and Wong*, 2002] affecting the frictional balance and slightly affecting water level. Lateral changes in bathymetry over the cross section of the bay alter the pressure gradient balance in the bay affecting water level and currents [*Csanady*, 1973; *Signell et al*., 1990]. Additionally, wave setup associated with intense wind events (e.g., nor'-easters and hurricanes) might be present offshore along the coast and can also be transferred into the bays and enhance water level response in the bay interior [*Olabarrieta et al*., 2011]. During intense storm events, the barrier island might overtop (overwash) resulting in additional transfer from the ocean into the bays. Under these conditions, the assumption of inlet dynamics being the only constraint to the flow into the bay will no longer be valid.

7.6. Sea Level Rise Considerations

While several processes control offshore sea level (tides, wind, current, and pressure systems), long-term sea level rise [*Douglas*, 1991; *Church and White*, 2006; *Ezer*, 2013] has a larger effect on the response of barrier islands to water level. Published sea level rise rates at a nearby station (New York The Battery), range from 5 mm yr^{-1} for the long-term rate, to 8 mm yr^{-1} for the trend after the year 2000 [*Ezer*, 2013]. The bay water level trend for the period 2007–2015 was 6.3 mm yr^{-1} at LIN, while at SH was 7.4 mm yr^{-1} (compared to the estimates of 13.5 mm yr^{-1} at LIN and 10.6 mm yr^{-1} at SH for 2007–2013 in *Aretxabaleta et al*. [2014]). The reduced trend in water level rise was a result of a drop in 2015 that can be at least partially explained by the effects of the intense 2014–2015 El Niño. When the rates were calculated for 2007–2014 (excluding the 2015 data), the rates were 11.8 mm yr^{-1} at LIN and 9.3 mm yr^{-1} at SH. The relatively short-term trends calculated need to be taken with caution as sea levels along the northeast show significant year-to-year fluctuations [*Goddard et al*., 2015] and can result in overestimations of sea level rise rates. However, these rates are consistent with recent trend estimates in the MAB [*Church and White*, 2006; *Ezer*, 2013] and are faster than the global rate of sea level rise [*Douglas*, 1991; *Sallenger et al*., 2012]. The magnitudes of the changes in M2 tidal amplitudes (order 0.02 m) during the 8 year study period were about one-third the changes caused by sea level rise (order 0.06 m).

8. Summary

The water level response in semienclosed bays in southern Long Island, New York to offshore forcing was explored using observations from several water level stations and an analytical model. The main drivers of water level fluctuations in the bays are offshore tides, storm surge, and longer-term changes such as sea level rise. The area of the bay and the number and size of the connections with the offshore determine the magnitude of the transfer of offshore fluctuations into the bays. Fluctuations at tidal frequencies were reduced in bays with large areas and small connections (e.g., Great South Bay) and sometimes enhanced in

small area bays with large connections (e.g., Jamaica Bay). The transfer of low-frequency fluctuations in all bays was near unity and thus long-term sea level rise was fully transmitted into the back-barrier bays. In the analyzed period, the average response of the bays is independent of the magnitude of the offshore fluctuations at a specific frequency.

Changes in M_2 tidal constituent amplitudes following intense storms, such as Hurricanes Irene and Sandy, were small. A ten percent increase in the M_2 tidal amplitude at Lindenhurst ($\sim$0.02 m) in spring 2014, coincided with dredging in nearby Fire Island Inlet and Jones Inlet and occurred during an increase in cross section of the Wilderness Breach. The relative importance of the near-simultaneous geomorphological changes in bay water level after December 2012 was difficult to separate. An increase of 0.01 m in April 2008 occurred following dredging of Fire Island and Jones Inlet. These observations suggest dredging can increase the amplitude of the M_2 tide in these back-barrier bays. The sea level rise-induced increase in water level exceeded 0.06 m during the period 2007–2015, 3 times larger than observed fluctuations in M_2 amplitude. Enhanced transfer (at most frequencies) between the offshore and bays, especially in Great South Bay and the areas surrounding Jones Inlet occurred during and following geomorphic changes (e.g., dredging) within the bays and inlets.

An analytical model, based on the balance between friction and pressure gradient in the inlet, predicts the transfer of offshore sea level fluctuations to back-barrier bays as a function of the size of the inlets, the area of the bays, and friction in the inlets. The model was matched to the observed transfer from offshore at most spectral frequencies by adjusting the value of the linearized friction. The model is applicable to any bay system for which inlet friction acts as the main controlling factor of the water level exchange into the bays. An expanded model that included the multiple connections with the offshore and between the bays was developed and allowed for estimates of the transfer response in Moriches and Shinnecock bays, where observations were unavailable. The model provides a simple framework for the study of the water level changes in back-barrier bays caused by changes in geomorphology, storm events, and sea level rise.

Acknowledgments

The authors thank Bill Schwab (USGS) and Steve Lentz (WHOI) for helpful comments and suggestions. Fire Island Inlet and Jones Inlet dredging information was obtained from the U.S. Army Corps of Engineers (http://www.nan.usace.army.mil/Media/Fact-Sheets/Fact-Sheet-Article-View/Article/487607/fact-sheet-fire-island-inlet-and-shores-westerly-to-jones-inlet-new-york/, http://www.nan.usace.army.mil/Media/News-Stories/Story-Article-View/Article/488061/us-army-corps-of-engineers-completes-jones-inlet-project/) and from the New York State Department of Environmental Conservation (NYS-DEC). We are grateful for the assistance of Anna Servidone at NYS-DEC. Cross-sectional area of the Wilderness Breach was obtained from Stony Brook State University of New York (http://po.msrc.sunysb.edu/GSB/, Inlet Report 14). The data used are listed in the references, tables, supplements, and the repository at http://waterdata.usgs.gov/nwis/inventory/?site_no=xxx, where xxx stands for the USGS station number in Table 1. Any use of trade, firm, or product names is for descriptive purposes only and does not imply endorsement by the U.S. Government.

References

Arbic, B. K., P. St-Laurent, G. Sutherland, and C. Garrett (2007), On the resonance and influence of the tides in Ungava Bay and Hudson Strait, *Geophys. Res. Lett.*, *34*, L17606, doi:10.1029/2007GL030845.

Aretxabaleta, A. L., B. Butman, and N. K. Ganju (2014), Water level response in back-barrier bays unchanged following Hurricane Sandy, *Geophys. Res. Lett.*, *41*, 3163–3171, doi:10.1002/2014GL059957.

Bendat, J. S., and A. G. Piersol (1986), *Random Data. Analysis and Measurement Procedures*, 566 pp., John Wiley, New York.

Brownell, A. T., C. J. Hapke, N. J. Spore, and J. E. McNinch (2015), Bathymetry of the wilderness breach at Fire Island, New York, June 2013, *U.S. Geol. Surv. Data Ser. 914*, Reston, Va., doi:10.3133/ds914.

Butman, B., P. S. Alexander, C. K. Harris, F. S. Lightsom, M. A. Martini, M. B. Ten Brink, and P. A. Traykovski (2003), Oceanographic observations in the Hudson Shelf Valley, December 1999 - April 2000: Data Report [DVD-ROM], *U.S. Geol. Surv. Open File Rep., 02-217*.

Cañizares, R., and J. L. Irish (2008), Simulation of storm-induced barrier island morphodynamics and flooding, *Coastal Eng.*, *55*(12), 1089–1101.

Chuang, W.-S., and E. M. Swenson (1981), Subtidal Water level variations in Lake Pontchartrain, Louisiana, *J. Geophys. Res.*, *86*(C5), 4198–4204, doi:10.1029/JC086iC05p04198.

Church, J. A., and N. J. White (2006), A 20th century acceleration in global sea-level rise, *Geophys. Res. Lett.*, *33*, L01602, doi:10.1029/2005GL024826.

Csanady, G. T. (1973), Wind-induced barotropic motions in long lakes, *J. Phys. Oceanogr.*, *3*, 429–438.

Csanady, G. T. (1981), Circulation in the coastal ocean, *Adv. Geophys.*, *23*, 101–183.

Douglas, B. C. (1991), Global sea level rise, *J. Geophys. Res.*, *96*(C4), 6981–6992, doi:10.1029/91JC00064.

Ezer, T. (2013), Sea level rise, spatially uneven and temporally unsteady: Why the U.S. East Coast, the global tide gauge record, and the global altimeter data show different trends, *Geophys. Res. Lett.*, *40*, 5439–5444, doi:10.1002/2013GL057952.

Forrester, W. D. (1986), Direct inference of tidal constituents, *Int. Hydrogr. Rev.*, *63*(2), 109–110.

Freeman, N. G., R. F. Hamblin, and T. S. Murty (1974), Helmholtz resonance in harbors of the Great Lakes, in *Seventeenth Conference on Great Lakes Research*, pp. 399–411, Int. Assoc. for Great Lakes Res., Hamilton, Ontario, Canada.

Garrett, C. (1972), Tidal resonance in the Bay of Fundy and Gulf of Maine, *Nature*, *238*, 441–443.

Garvine, R. W. (1985), A simple model of estuarine subtidal fluctuations forced by local and remote wind stress, *J. Geophys. Res.*, *90*(C6), 11,945–11,948.

Goddard, P. B., J. Yin, S. M. Griffies, and S. Zhang (2015), An extreme event of sea-level rise along the Northeast coast of North America in 2009–2010, *Nat. Commun.*, *6*, 6346, doi:10.1038/ncomms7346.

Hartig, E. K., V. Gornitz, A. Kolker, F. Mushacke, and D. Fallon (2002), Anthropogenic and climate-change impacts on salt marshes of Jamaica Bay, New York City, *Wetlands*, *22*(1), 71–89.

Irish, J. L., and R. Cañizares (2009), Storm-wave flow through tidal inlets and its influence on bay flooding, *J. Waterw. Port Coastal Ocean Eng.*, *135*(2), 52–60.

Janzen, C. D., and K.-C. Wong (2002), Wind-forced dynamics at the estuary-shelf interface of a large coastal plain estuary, *J. Geophys. Res.*, *107*(C10), 3138, doi:10.1029/2001JC000959.

Johnson, M. C. (1983), *Fire Island, 1650s-1980s*, 214 pp., Shoreland Press, Mountainside, N. J.

Keulegan, G. H. (1967), Tidal flow in entrances: Water-level fluctuations of basins in communication with seas. Committee on Tidal Hydraulics, *Tech. Bull*. *14*, 89 pp., U.S. Army Corps of Eng., Vicksburg, Miss.

Kowalik, Z., and T. S. Murty (1993), *Numerical Modeling of Ocean Dynamics*, *Advanced Series on Ocean Engineering*, vol. 5, 485 pp., World Sci., Singapore. [Available at http://www.worldscientific.com/worldscibooks/10.1142/1970.]

Lentz, S., R. T. Guza, S. Elgar, F. Feddersen, and T. H. C. Herbers (1999), Momentum balances on the North Carolina inner shelf, *J. Geophys. Res.*, *104*(C8), 18205–18226, doi:10.1029/1999JC900101.

Nicholls, R. J., P. P. Wong, V. R. Burkett, J. O. Codignotto, J. E. Hay, R. F. McLean, S. Ragoonaden, and C. D. Woodroffe (2007), Coastal systems and low-lying areas, in *Climate Change 2007: Impacts, Adaptation and Vulnerability, Contribution of Working Group II to the Fourth Assessment Report of the Intergovernmental Panel on Climate Change*, edited by M. L. Parry et al., Cambridge Univ. Press, Cambridge, U. K.

NYCDEP (2007), Jamaica Bay Watershed Protection Plan Volume I—Regional Profile, 131 pp., New York. [Available at http://www.nyc.gov/html/dep/pdf/jamaica_bay/vol-1-complete.pdf.]

Olabarrieta, M., J. C. Warner, and N. Kumar (2011), Wave-current interaction in Willapa Bay, *J. Geophys. Res.*, *116*, C12014, doi:10.1029/2011JC007387.

Orton, P. M., S. A. Talke, D. A. Jay, L. Yin, A. F. Blumberg, N. Georgas, H. Zhao, H. J. Roberts, and K. MacManus (2015), Channel shallowing as mitigation of coastal flooding, *J. Mar. Sci. Eng.*, *3*(3), 654–673.

Pawlowicz, R., R. C. Beardsley, and S. Lentz (2002), Classical tidal harmonic analysis including error estimates in MATLAB using T-TIDE, *Comput. Geosci.*, *28*, 929–937.

Sallenger, A. H., Jr., K. S. Doran, and P. A. Howd (2012), Hotspot of accelerated sea-level rise on the Atlantic coast of North America, *Nat. Clim. Change*, *2*(12), 884–888.

Schwab, W. C., W. E. Baldwin, C. J. Hapke, E. E. Lentz, P. T. Gayes, J. F. Denny, J. List, and J. C. Warner (2013), Geologic evidence for onshore sediment transport from the inner continental shelf: Fire Island, New York, *J. Coastal Res.*, *29*(3), 526–544.

Schwab, W. C., W. E. Baldwin, and J. F. Denny (2016), Assessing the impact of Hurricanes Irene and Sandy on the morphology and modern sediment thickness on the inner continental shelf offshore of Fire Island, New York, *U.S. Geol. Surv. Open File Rep., 2015–1238*, 15 pp. [Available at http://dx.doi.org/10.3133/ofr20151238.]

Scott, J. T., and G. T. Csanady (1976), Nearshore currents off Long Island, *J. Geophys. Res.*, *81*(30), 5401–5409.

Signell, R. P., R. C. Beardsley, H. C. Graberand, and A. Capotondi (1990), Effect of wave-current interaction on wind-driven circulation in narrow, shallow embayments, *J. Geophys. Res.*, *95*(C6), 9671–9678.

Sorensen, R. M., and W. N. Seelig (1977), Hydraulics of Great Lakes inlet-harbor systems, in *Proceedings of Fifteenth Coastal Engineering Conference*, vol. 2, pp. 1646–1665, Am. Soc. of Civ. Eng., Honolulu, Hawaii.

Spaulding, M. L. (1994), *Modeling of Circulation and Dispersion in Coastal Lagoons. Coastal Lagoon Processes*, *Elsevier Oceanogr. Ser.*, *60*, 103–131.

Sutherland, G., C. Garrett, and M. Foreman (2005), Tidal resonance in Juan de Fuca Strait and the Strait of Georgia, *J. Phys. Oceanogr.*, *35*, 1279–1286.

Swanson, R. L., and R. E. Wilson (2008), Increased tidal ranges coinciding with Jamaica Bay development contribute to marsh flooding, *J. Coastal Res.*, *24*, 1565–1569.

U.S. Army Corps of Engineers (2001), Fire Island Inlet to Montauk Point Reformulation Study, Breach/Overwash Position Paper, NY District, 52 pp., New York. [Available at http://www.nan.usace.army.mil/Portals/37/docs/civilworks/projects/ny/coast/fimp/2001.pdf.]

Van Ormondt, M., C. Hapke, D. Roelvink, and T. Nelson (2015), The effects of geomorphic changes during Hurricane Sandy on water levels in Great South Bay, in *The Proceedings of the Coastal Sediments 2015*, 14 pp., World Sci., Singapore.

Wong, K.-C., and J. DiLorenzo (1988), The response of Delaware's inland bays to ocean forcing, *J. Geophys. Res.*, *93*(C10), 12,525–12,535.

Wong, K.-C., and J. E. Moses-Hall (1998), On the relative importance of the remote and local wind effects to the subtidal variability in a coastal plain estuary, *J. Geophys. Res.*, *103*(C9), 18,393–18,404.

Wong, K.-C., and R. E. Wilson (1984), Observations of low-frequency variability in Great South Bay and relations to atmospheric forcing, *J. Phys. Oceanogr.*, *14*, 1893–1900.